Hindawi
International Journal of Antennas and Propagation
Volume 2018, Article ID 8737594, 10 pages
https://doi.org/10.1155/2018/8737594

Research Article

Diffraction Loss Prediction of Multiple Edges Using Bullington Method with Neural Network in Mountainous Areas

Changwon Lee and Sungkwon Park

Department of Electronics and Computer Engineering, Hanyang University, Seoul 133-791, Republic of Korea

Correspondence should be addressed to Sungkwon Park; sp2996@hanyang.ac.kr

Received 30 September 2017; Revised 25 December 2017; Accepted 31 December 2017; Published 25 February 2018

Academic Editor: Lorenzo Luini

This paper proposes a neural network approach to improve the Bullington method by using parameters obtained from ignored obstacles in mountainous areas. Measurements were performed in mountainous areas to compare the prediction accuracy of propagation loss. And the measured data were used for neural network training. A detailed description of the input parameters of the proposed neural network is presented. The prediction performances were improved by up to 3.20 dB in the average error and 2.11 dB in the standard deviation of errors by the proposed method when compared to traditional diffraction methods.

1. Introduction

Propagation loss prediction is one of the main problems in planning of radio communication links. And it is also very important to design mobile radio systems [1]. In Korea, the mountainous area is about 70% of the whole land area and the hilly terrain can cause multiple obstacles to the signal path. In hilly terrains, line-of-sight propagation is not possible at all the places and the diffraction becomes dominant on propagation [2]. However, accurate prediction of the diffraction losses is still challenging for realistic propagation environments such as mountainous regions [3]. Practically simplified models are used such as Bullington, Deygout, Causebrook, and Giovanelli for computational efficiency [3, 7]. Those models use knife edges to replace the mountain peaks and ridges for computing diffraction losses [2, 3]. In contrast, more sophisticated techniques such as UTD (uniform theory of diffraction) can be used to improve accuracy but need much more computation time and detailed information of terrains and obstacles such as conductivity of the materials [4].

Here, we propose a neural network with Bullington model in the presence of three or more edges. To improve the prediction accuracy of diffraction loss, the proposed method uses ignored edges in the Bullington method to calculate additive diffraction losses. Parameters obtained from terrain elevation information were used as inputs to the neural network. The details are described in Section 3.

Measurements were conducted in mountainous areas. The measured data were used to evaluate the diffraction loss prediction and train the neural network using training algorithm.

The structure of this paper is as follows. Section 2 introduces the traditional diffraction models. And the proposed method and training are described in Sections 3 and 4, respectively. Section 5 illustrates the measurement campaign. Section 6 gives the evaluation of the prediction performance. Conclusions are drawn in Section 7.

2. Diffraction Methods

2.1. Bullington Method. In the Bullington method, the real terrain is reduced to a single equivalent knife edge. The location of the equivalent knife edge is the point at which the extended lines joining the transmitter and receiver to their respective dominant (the greatest angle of elevation as viewed from transmitter or receiver) obstacles meet as shown in Figure 1 [5]. Then the diffraction loss is computed using (1) and (2) [4, 6]. This method has the advantage of simplicity

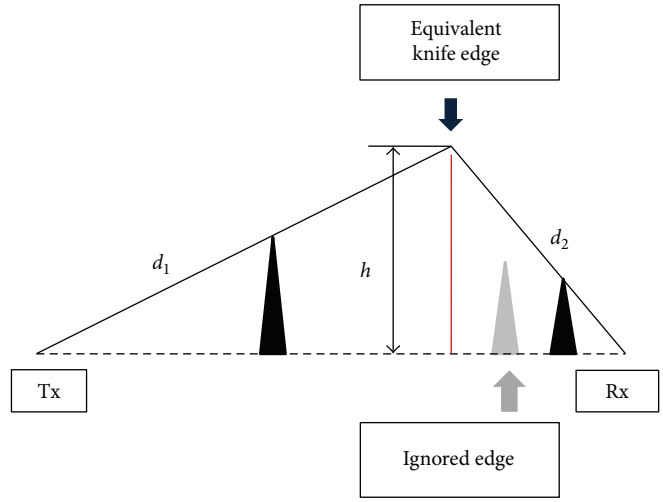

Figure 1: Concept of Bullington method.

but obstacles below the paths of the horizon rays can be ignored. And this may cause large prediction errors. In general, it underestimates path losses [4, 5].

The geometrical parameters are combined in a dimensionless parameter denoted by ν as shown in [6]:

$$\nu = h\sqrt{\frac{2}{\lambda}\left(\frac{1}{d_1}+\frac{1}{d_2}\right)}, \quad (1)$$

where h is the height of the top of the obstacle above (or below) the straight path line and d_1 and d_2 are the distances of the path ends from the top of the obstacle. If the obstacle is below the straight path line, then h is negative. The diffraction loss as a function of ν is presented in (2) for ν greater than -0.78 [6]. It should be noted that the diffraction loss can be avoided for $\nu \le -0.78$ [6].

$$J(\nu) = 6.9 + 20\log\left(\sqrt{(\nu-0.1)^2+1}+\nu-0.1\right)(\text{dB}). \quad (2)$$

The approximated diffraction loss, L_B, due to the equivalent Bullington edge is equal to (2), and the total path loss using the Bullington method is [4]

$$L_p = L_{fs} + L_B(\text{dB}), \quad (3)$$

where L_{fs} is free space loss [16].

2.2. Deygout Method. The Deygout method is drawn in Figure 2 for a path with three obstacles. The first step is to compute ν parameter using (1) for each edge alone, as if all other edges were absent, that is, all ν parameters are calculated for the paths Tx-A-Rx, Tx-B-Rx, and Tx-C-Rx in Figure 2. If edge B is the main edge in Figure 2, then the diffraction losses, which are $J(\nu_{D\_A})$ and $J(\nu_{D\_C})$, for edge A and edge C are found with respect to a line joining the main edge to the Tx and Rx. And those are added to the main edge loss ($J(\nu_{D\_B})$) to obtain a total approximated diffraction loss (L_D), by Deygout method [4, 7]. The diffraction loss at each edge is calculated using (2). The total path loss using the Deygout

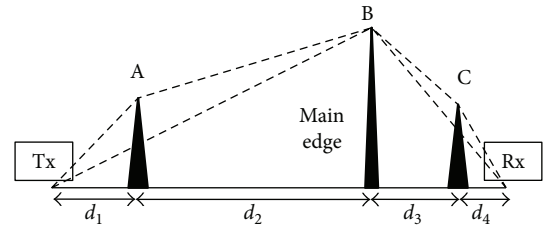

Figure 2: Concept of Deygout method.

method is presented in (4) [4]. This procedure can be repeated until all the edges have been considered for more than three edges [4, 8]. However, it is common to compute the total loss as the sum of one main edge and two subsidiary main edges on either side in practical applications [4, 8].

$$L_p = L_{fs} + L_D(= J(\nu_{D\_B}) + J(\nu_{D\_A}) + J(\nu_{D\_C}))(\text{dB}), \quad (4)$$

where L_{fs} is free space loss [16].

2.3. Causebrook Method (Correction). To reduce an overestimation problem of the Deygout method, Causebrook proposed an approximate correction derived from the exact analysis of the two-edge solution [24]. The corrected form is given in

$$L_{\text{Corrected}} = L_p - C_1 - C_2(\text{dB}), \quad (5)$$

where L_D is the diffraction loss from (4). The correction factors C_1 and C_2 are presented below [24]:

$$C_1 = (6 - L_2 + L_1)\cos\alpha_1,$$
$$C_2 = (6 - L_2 + L_3)\cos\alpha_2, \quad (6)$$

where $\cos\alpha_1 = \sqrt{d_1(d_3+d_4)/(d_1+d_2)(d_2+d_3+d_4)}$, $\cos\alpha_3 = \sqrt{(d_1+d_2)d_4/(d_1+d_2+d_3)(d_3+d_4)}$, and L_1 and L_3 are the losses due to edges A and C, as if they existed on their own between the Tx and Rx. And d_1, d_2, d_3, and d_4 are shown in Figure 2.

2.4. Giovanelli Method. Another development of the Deygout method has been proposed [24, 25]. The concept for the Giovanelli method is shown in Figure 3. It is assumed that edge A is the main edge in this case. Then a reference field point F′ is found by projecting AB onto F′F″ and h_1'' is defined in [24]

$$h_1'' = h_1 - \frac{d_1 H}{d_1 + d_2 + d_3}, \quad (7)$$

where $H = h_2 + md_3$ and $m = (h_2 - h_1)/d_2$. The effective height for the secondary edge B is then given by [24]

$$h_2'' = h_2 - \frac{d_3 h_1}{d_2 + d_3}. \quad (8)$$

The total diffraction loss is now given in [24]

$$L_{GV} = J\left(\nu\left(d_1, d_2 + d_3, h_1''\right)\right) + J\left(\nu\left(d_2, d_3, h_2''\right)\right)\ (\text{dB}), \quad (9)$$

where J(·) is the loss from (2). This method is conveniently extended to more than two edges by recursively applying the above procedure [24].

3. Proposed Method

As mentioned in Section 2, there may be ignored edges in the Bullington method, which generally cause underestimation. Therefore, for multiple edges on the path, we propose a method to obtain the total diffraction loss by adding the loss from the Bullington method and the loss from the ignored edges. Where the diffraction loss from the ignored edges is calculated using a neural network as shown in Figure 4. There are 15 inputs of the proposed neural network, all of which can be obtained from DTM (digital terrain model). Inputs 1 through 9 are consisted of the heights of Tx and Rx, the three largest ν of ignored obstacles, the distances between Tx and three ignored obstacles, and the distance of the total path. Inputs 10 through 15 are approximate front and rear slopes of ignored edges. An approximate slope is calculated as the height difference between the edge and the point spaced by 30 m from the edge as shown in Figure 5. The use of slopes is intended to improve the prediction performance by considering the obstacle radius of curvature [9, 10]. This is an approximate application for the obstacle radius of curvature in the diffraction loss calculation. The proposed method is applied when there are at least three edges to include an ignored edge on the paths. For paths with three or more edges, the prediction of the proposed method is compared with the two traditional diffraction methods in Section 2, and the results are presented in Section 6.

4. Training

Figure 6 shows a simple neuron. The neuron is presented with inputs as shown in

$$\mathbf{x} = \begin{bmatrix} x_1 & x_2 & \cdots & x_n \end{bmatrix}^T, \quad (10)$$

and an output value of a neuron is produced as shown in [11]

$$\text{net} = \mathbf{w}^T \mathbf{x}, \quad (11)$$

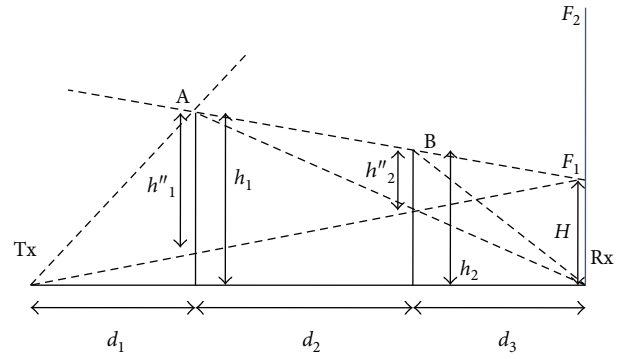

Figure 3: Concept of Giovanelli method.

where $(\cdot)^T$ denotes the transpose, and the weights of a neuron $\mathbf{w}$ are presented in

$$\mathbf{w} = \begin{bmatrix} w_1 & w_2 & \cdots & w_n & \text{b} \end{bmatrix}^T. \quad (12)$$

The activation function has been selected to be the commonly used hyperbolic tangent sigmoid transfer function [11]. Figure 7 shows the architecture of the neural network with inputs of the proposed method. The inputs in Figure 7 correspond to those shown in Figure 5. Prior to training, data with three or more obstacles should be extracted from all of the measurement data. And it is necessary to divide all the measurement data with three or more edges into each of the two disjoint sets which are training and testing sets. The training sets are only used in the training procedure, and the testing sets are used for the evaluation of prediction performances. The training data are randomly chosen to be about 50% of the measurement data with three or more edges in this paper. The input vectors shown in Figures 5 and 7 can be obtained from the DTM corresponding to the transmitting and the receiving positions as described in Section 3. The receiving power may be expressed in (13) in wireless environments [12, 13].

$$P_\text{r} = P_\text{t} + G_\text{t} + G_\text{r} - L_\text{p}(\text{dBm}), \quad (13)$$

where P_t is the transmitting power, G_t and G_r are the gains of the Tx and Rx antennas. L_p is the path loss. Bullington proposed that the diffraction loss has to be added to the free space loss when the path is obstructed [4, 14, 15]. In order to find target values, (14) can be obtained from (13) by using the Bullington method as shown in (3).

$$P_\text{r} = P_\text{t} + G_\text{t} + G_\text{r} - L_\text{fs} - L_\text{B} - L_\text{t}(\text{dB}), \quad (14)$$

where L_fs is the free space loss and L_B is the Bullington diffraction loss. L_t is the target value, which is desired loss due to ignored edges for training. The target value can be obtained using (14) where P_r is measured power in dBm, G_t and G_r are 2.15 dBi gain, and P_t is 36 dBm as drawn in Figure 8. And the free space loss L_fs is computed using [16]

$$L_\text{fs} = 32.4 + 20\log f + 20\log d(\text{dB}), \quad (15)$$

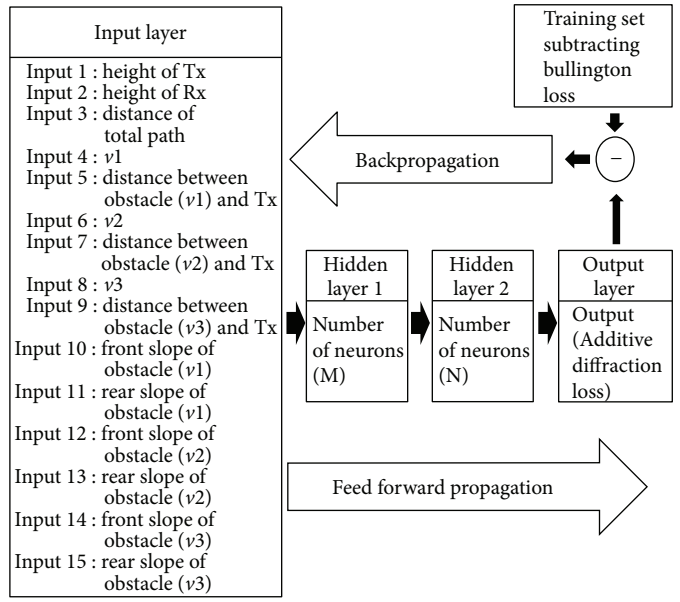

Figure 4: Architecture of the proposed method.

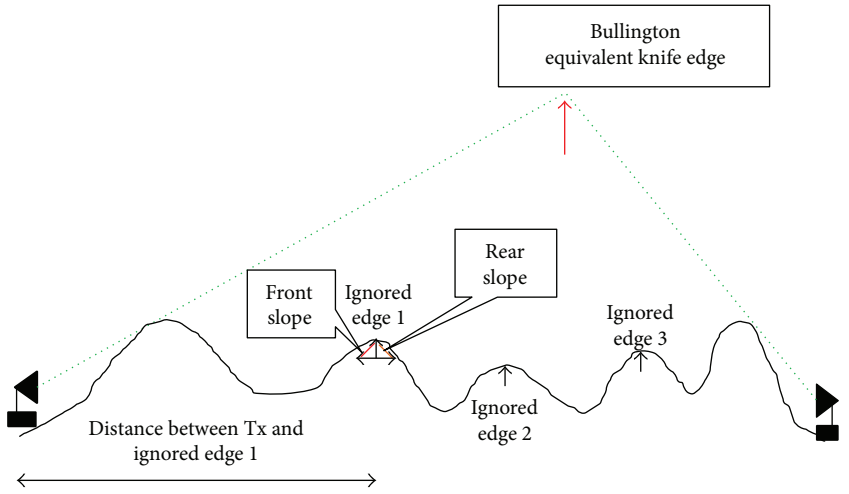

Figure 5: Slopes of an ignored edge.

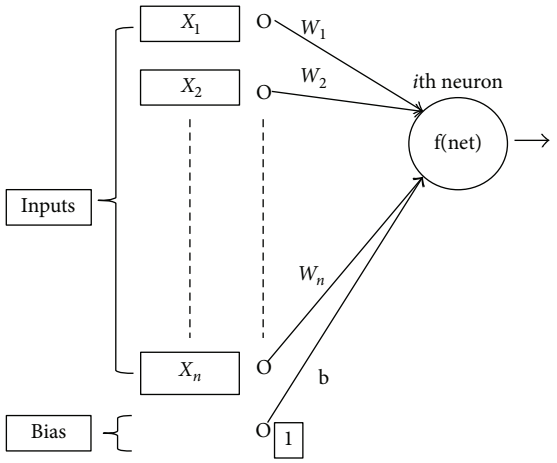

Figure 6: Neuron model.

where f is the frequency (MHz) and d is distance (km).

Here, the error is defined for the feed-forward neural network as shown in

$$e_{\mathrm{NN}}(j) = o(j) - L_{\mathrm{t}}(j)(\mathrm{dB}), \tag{16}$$

where o(j) is the output of the neural network corresponding to an input vector, $L_{\mathrm{t}}(j)$ is a target value, and j is the index number of training data. In the backpropagation procedure, the weights of the neural network are adjusted by minimizing the mean square error as follows.

$$\mathrm{MSE} = \frac{1}{N}\sum_{j=1}^{N} e_{\mathrm{NN}}^2(j). \tag{17}$$

The Levenberg-Marquardt algorithm [17] is used to update the weights of the proposed neural network. The

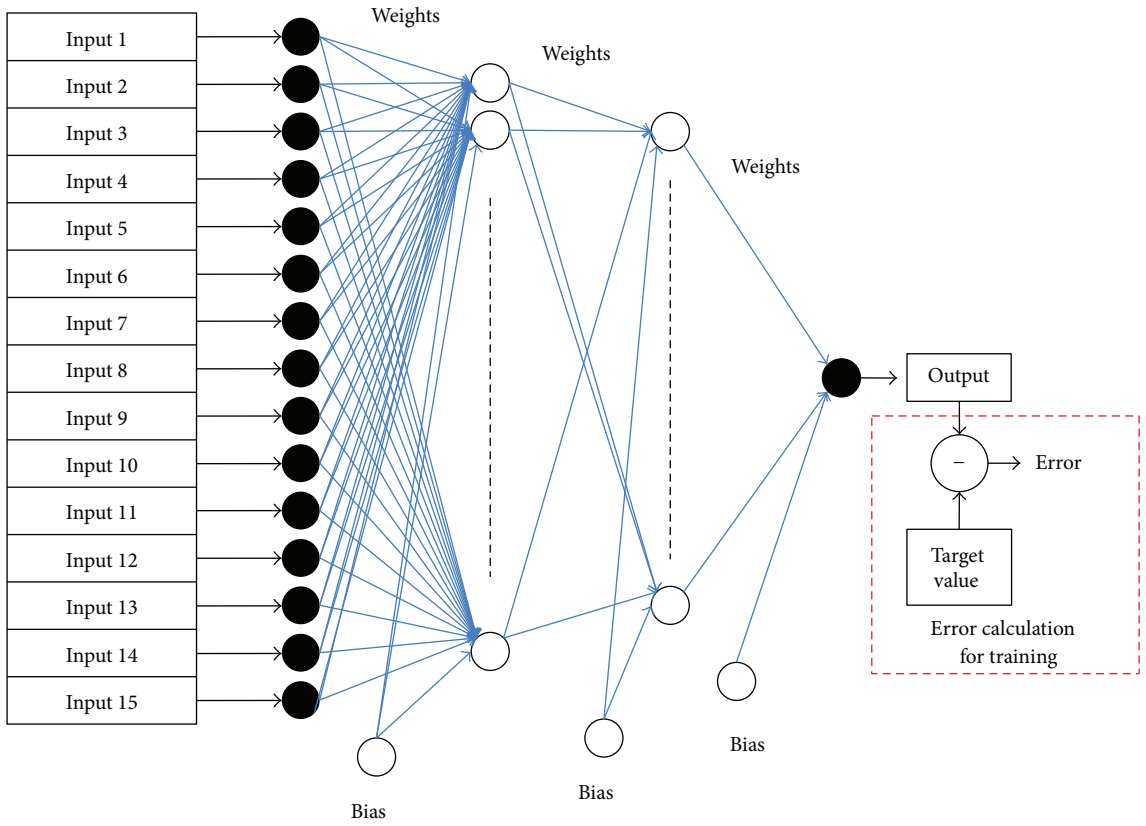

Figure 7: Diagram of the proposed method.

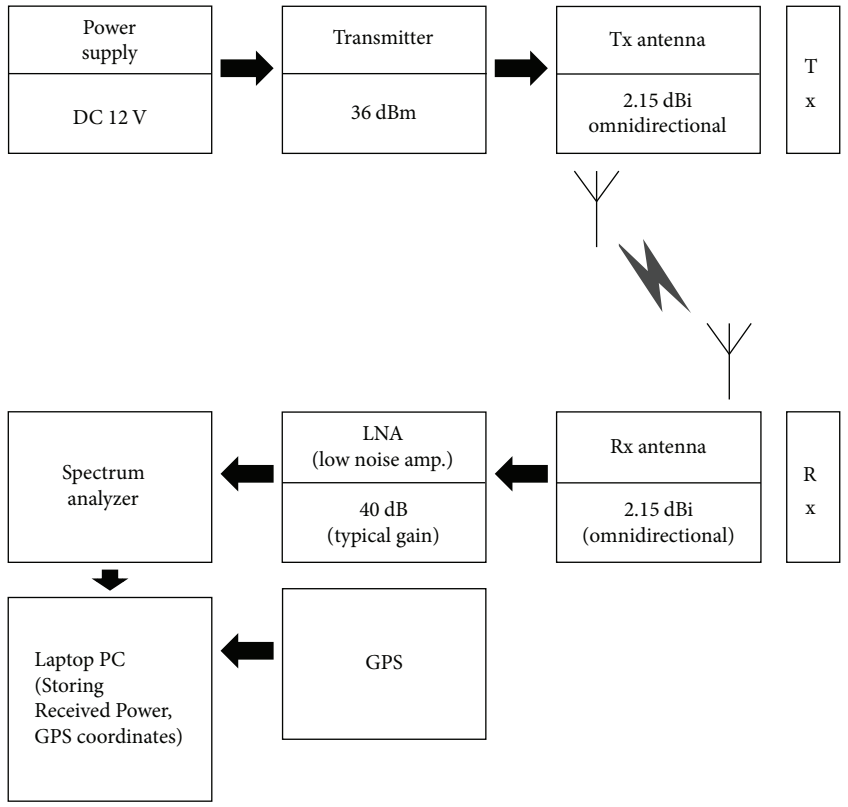

Figure 8: Measurement configuration diagram.

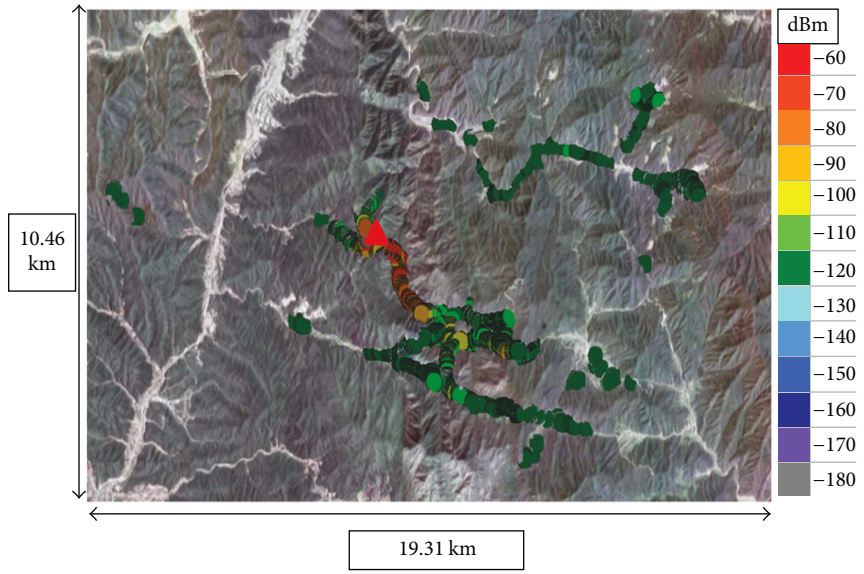

Figure 9: Measurements in the west side of Mt. Maebong.

algorithm has been introduced to training neural networks faster than the standard gradient descent backpropagation algorithm by more than 10 times [18, 19]. In the trials of many cases, the numbers of neurons in the hidden layers with the best results are $N = 20$ and $M = 12$. In the procedure of the backpropagation training, the epochs are as follows: 109 epochs and 128 epochs for the west side of Mt. Maebong and Mt. Ongma, respectively, in Figures 9 and 10.

5. Measurement Campaign

Measurements have been performed in the three mountain areas as shown in Figures 9–11. The heights of the selected mountains for measurement purposes are as follows: 746.7 m, 533.1 m, and 1420.2 m for the west side of Mt. Maebong in Inje, Mt. Ongma in Boryeong, and Mt. Hwaak in Gapyeong, respectively, in Figures 9–11. The selected mountains are typical hilly mountains in the Republic of Korea. In these mountains, it was convenient and safe to conduct measurements using a vehicle. The red triangle marks in Figures 9–11 are the transmitting positions, and the circles are measuring points. The total number of measurement data in Figures 9–11 is as follows: 80,163 for the west side of Mt. Maebong, 77,215 for Mt. Ongma, and 35,057 for Mt. Hwaak.

The transmitting signal is 1399 MHz continuous wave. This frequency was temporarily allowed in UHF band for the measurement campaign. The transmitting antenna is fixed on tripod of 6 m height, and the receiving antenna is placed on the roof of a car at a height of 1.8 meter above ground. The power of the transmitter is 36 dBm with a 2.15 dBi gain antenna and a cable of 2.71 dB loss. The measurement data are obtained from a spectrum analyzer connected to a 2.15 dBi gain antenna and a 40 dB gain low-noise-amplifier. A measurement configuration diagram is shown in Figure 8. The measurement data with three or more obstacles from the real mountain areas are used to produce train sets for the proposed method and later evaluate the performances

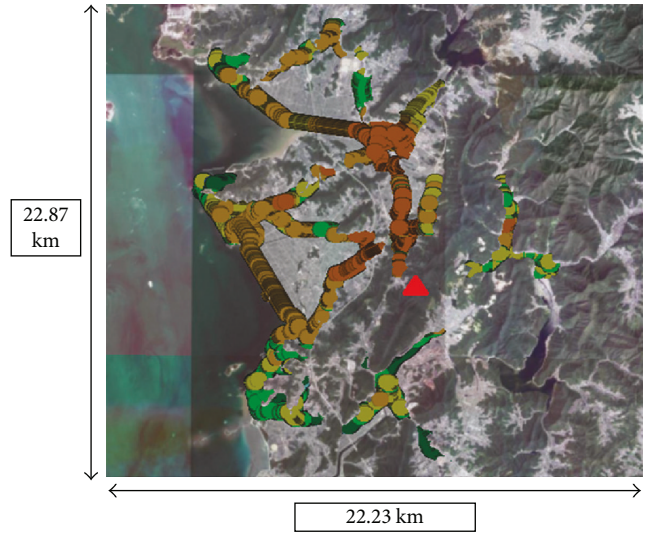

Figure 10: Measurements in Mt. Ongma.

of Bullington, Deygout, and the proposed method. The numbers of data with three or more obstacles are as follows: 1676, 5863, and 1147 for the west side of Mt. Maebong, Mt. Ongma, and Mt. Hwaak, respectively. And the numbers of training data are as follows: 838 and 2932 for the west side of Mt. Maebong and Mt. Ongma. And all training data consist of 70% for training and 30% for validation.

6. Comparison of Prediction Performance

The proposed method is applied to real mountainous environments. Two scenarios are discussed for the comparisons of diffraction methods in mountainous areas as shown in Figures 12–14. The details of the scenarios are drawn in Sections 6.1 and 6.2.

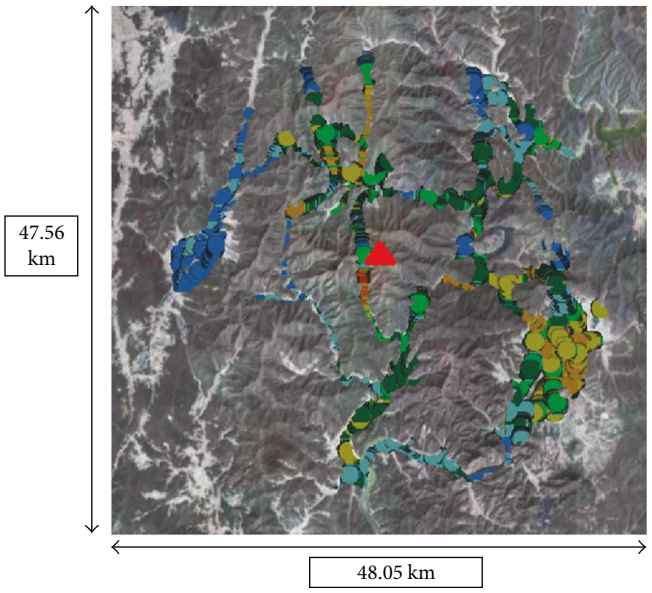

Figure 11: Measurements in Mt. Hwaak.

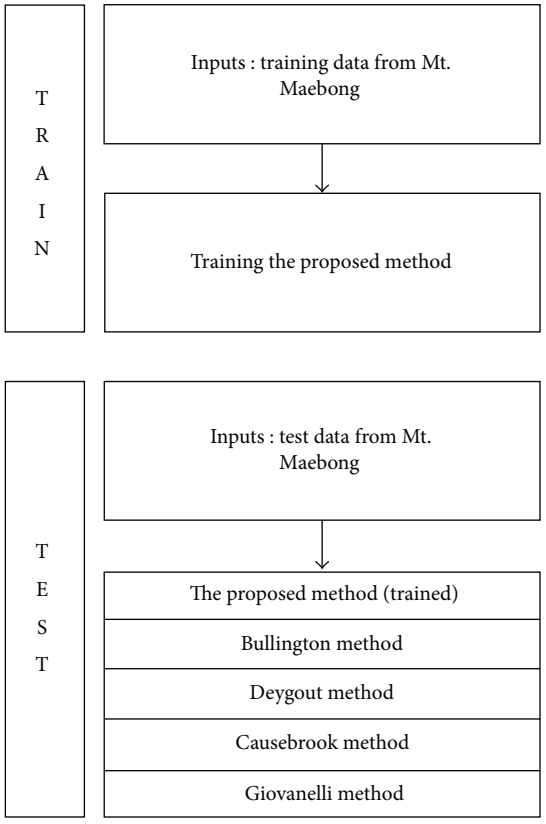

Figure 12: Scenario 1 (in Mt. Maebong).

In Section 6.1, the area-specific performance of the proposed method is investigated as shown in Figures 12 and 14. In Section 6.2, we try to find out the performance of the proposed method in another area as shown in Figure 14.

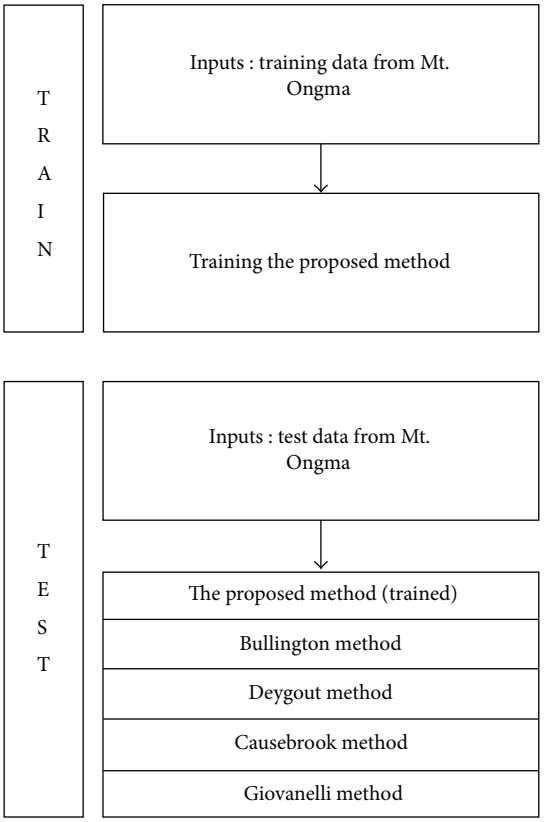

Figure 13: Scenario 1 (in Mt. Ongma).

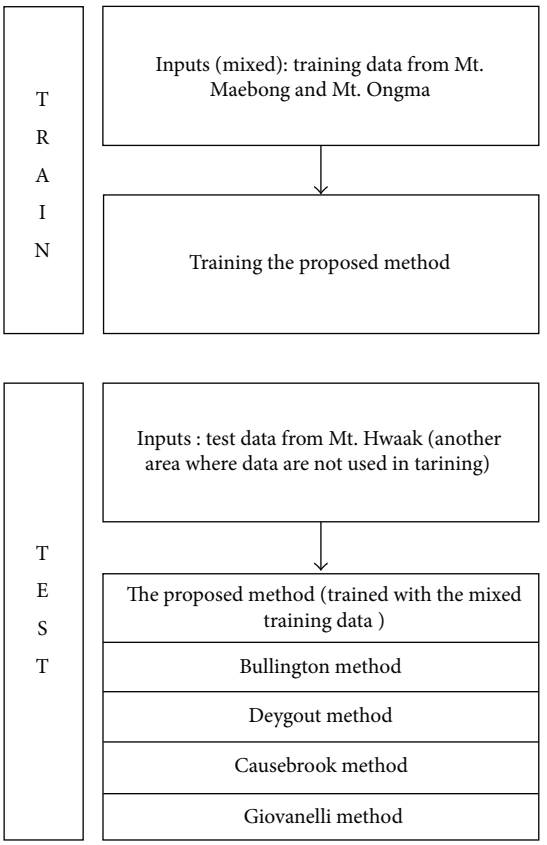

Figure 14: Scenario 2 (in Mt. Hwaak).

Table 1: Comparison of prediction performance.

Area	Method	Average error (dB)	Standard deviation of errors (dB)
Westside of Maebong mountain	Bullington	8.50	6.32
	Deygout	4.92	5.27
	Causebrook	3.53	5.19
	Giovanelli	4.86	5.25
	Proposed	2.75	4.66
Ongma mountain	Bullington	4.12	7.49
	Deygout	6.51	7.41
	Causebrook	7.17	7.51
	Giovanelli	6.45	7.42
	Proposed	0.92	5.30

6.1. Prediction Results of the Proposed Method with Traditional Methods. The proposed method is evaluated by comparing with the four diffraction methods described in Section 2. As described in Section 4, the testing sets are applied to the proposed method, Bullington method, Deygout method, Causebrook method, and Giovanelli method for the evaluation of prediction performances. The error is defined as shown in [2, 20, 21]

$$e(i) = p(i) - m(i)(\text{dB}), \tag{18}$$

where p is the prediction of received power, m is the measured value, and i is the point number of measurement data. The prediction values are obtained by using (14) with outputs of the neural network. The prediction values are calculated for each method as follows:

(1) Prediction values for the proposed method using (14)

$$p(i) = P_t + G_t + G_r - L_{fs}(i) - L_B(i) - o(i)(\text{dB}) \tag{19}$$

(2) Prediction values for the Bullington method using (3) and (13)

$$p(i) = P_t + G_t + G_r - L_{fs}(i) - L_B(i)(\text{dB}) \tag{20}$$

(3) Prediction values for the Deygout method using (4) and (13)

$$p(i) = P_t + G_t + G_r - L_{fs}(i) - L_D(i)(\text{dB}) \tag{21}$$

(4) Prediction values for the Causebrook method using (5) and (13)

$$p(i) = P_t + G_t + G_r - L_{fs}(i) - L_{\text{Corrected}}(i)(\text{dB}) \tag{22}$$

(5) Prediction values for the Giovanelli method using (9) and (13)

$$p(i) = P_t + G_t + G_r - L_{fs}(i) - L_{GV}(i)(\text{dB}) \tag{23}$$

The average error and the standard deviation of errors from (18) are considered to represent the prediction performance [22, 23].

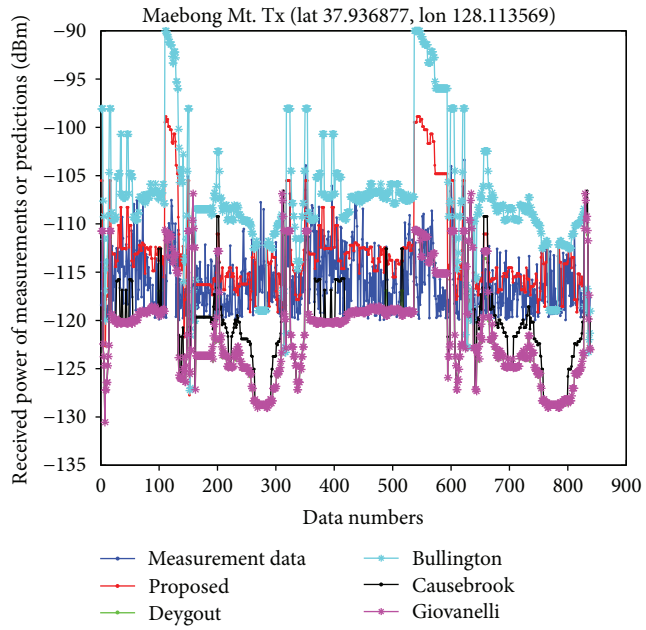

Figure 15: Comparison of the measurements and predictions in the west side of Mt. Maebong.

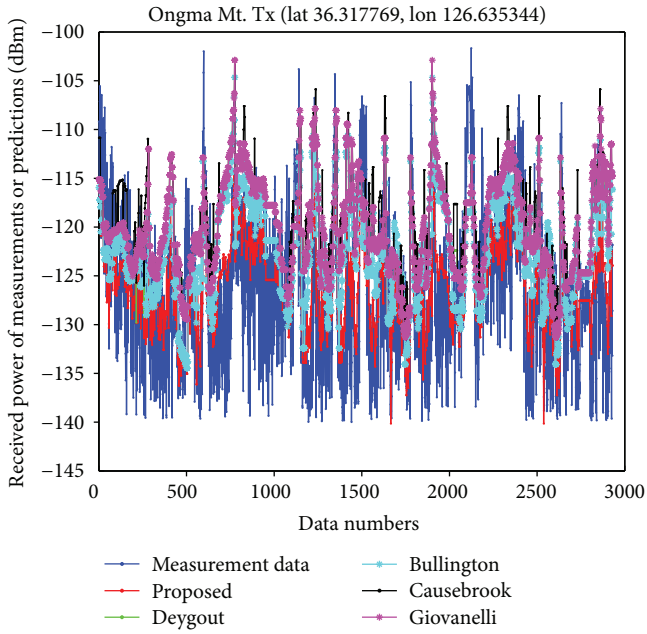

Figure 16: Comparison of the measurements and predictions in Mt. Ongma.

As described in Table 1 and Figures 15 and 16, the results show that prediction performances are improved when using the proposed method in mountain areas with three or more obstacles on the paths.

6.2. Prediction Results of the Trained Neural Network in the Area Where Data Are Not Used in Training. The proposed

Table 2: Comparison in the area where data are not used in training (Mt. Hwaak).

Area	Method	Average error (dB)	Standard deviation of errors (dB)
Hwaak mountain	Bullington	6.58	6.55
	Deygout	7.73	7.43
	Causebrook	9.45	7.45
	Giovanelli	8.11	6.83
	Proposed	0.71	5. 39

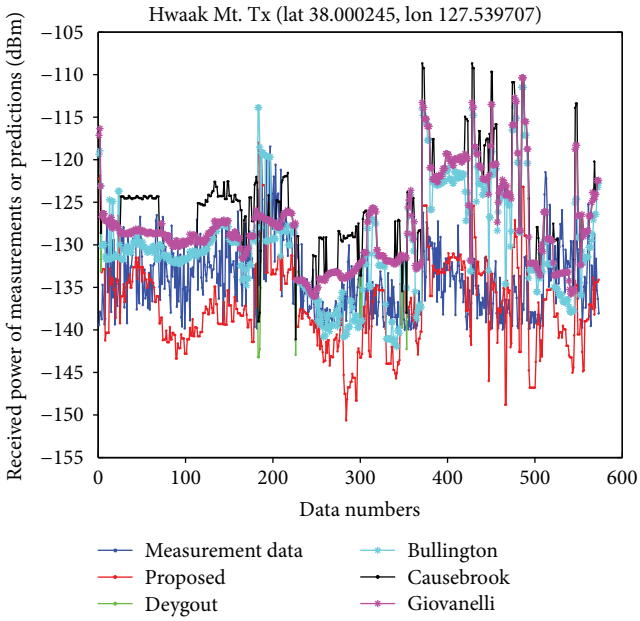

Figure 17: Comparison in the area where data are not used in training (Mt. Hwaak).

method which has been trained with measured data from Mt. Maebong and Mt. Ongma is applied to Mt. Hwaak as illustrated in Figure 14. To validate the pretrained neural network, the prediction accuracy is compared with Bullington, Deygout, Causebrook, and Giovanelli methods in the area where data are not used in training.

For the paths with three or more obstacles, neural network has been trained with all of the training data from the two areas in the previous subsection. The calculation for the prediction of each method uses (19), (20), (21), (22), and (23) as in Section 6.1. As shown in Table 2 and Figure 17, the comparison results show that prediction performance is improved by using the proposed method (pretrained neural network) in the area where data are not used in training.

7. Conclusion

A neural network-based diffraction method is proposed, and the method can be applied with the DTM in mountainous areas which have three or more obstacles on the paths. With a set of measured data of real mountain areas, the proposed method was evaluated with Bullington, Deygout, Causebrook, and Giovanelli methods and the results showed that the prediction performances were improved by up to 3.20 dB in the average error and 2.11 dB in the standard deviation of errors by the proposed method. The remaining results are shown in Table 1.

In addition, the prediction performance of the proposed method is validated by applying the proposed method which was trained with data from two areas to the area where data are not used in training. The results show that prediction performance is improved as described in Table 2. We used 838 data as minimum train set within about 10 km between Tx and Rx. To use the proposed method at longer distances, it is recommended to train the neural network with data from corresponding distances.

It is expected that the proposed method based on neural network would show better prediction results with more measurement data in hilly mountainous areas with multiple obstacles.

Conflicts of Interest

The authors declare that there is no conflict of interests regarding the publication of this paper.

Acknowledgments

This research was supported by the MSIP (Ministry of Science, ICT and Future Planning), Korea, under the ITRC (Information Technology Research Center) support program (IITP-2017-2012-0-00628) supervised by IITP (Institute for Information and Communications Technology Promotion).

References

[1] S. LeNgoc, J. Chen, T. Banerjee, and Y. Ye, "Improved diffraction loss prediction for land mobile radio communication," in *1994 Proceedings of Canadian Conference on Electrical and Computer Engineering*, pp. 242–247, Halifax, NS, Canada, 1994.

[2] T. R. Rao and S. V. Rao, "Single knife edge diffraction propagation studies over a hilly terrain," *IEEE Transactions on Broadcasting*, vol. 45, no. 1, pp. 20–29, 1999.

[3] D. A. Bibb, J. Dang, Z. Yun, and M. F. Iskander, "Computational accuracy and speed of some knife-edge diffraction models," in *2014 IEEE Antennas and Propagation Society International Symposium (APSURSI)*, pp. 705-706, Memphis, TN, USA, 2014.

[4] J. D. Parsons, *The Mobile Radio Propagation Channel*, John Wiley & Sons, 2nd edition, 2000.

[5] C. Haslett, *Essentials of Radio Wave Propagation*, Cambridge University Press, 2008.

[6] ITU-R, *Propagation by Diffraction, Recommendation ITU-R P.526–13*, 2013.

[7] C. Tzaras and S. R. Saunders, "Comparison of multiple-diffraction models for digital broadcasting coverage prediction," *IEEE Transactions on Broadcasting*, vol. 46, no. 3, pp. 221–226, 2000.

[8] H. R. Anderson, *Fixed Broadband Wireless System Design*, John Wiley & Sons, 2003.

[9] K. Hacking, "U.H.F. propagation over rounded hills," *Proceedings of the Institution of Electrical Engineers*, vol. 117, no. 3, pp. 499–511, 1970.

[10] H. T. Dougherty and L. J. Maloney, "Application of diffractions by convex surfaces to irregular terrain situations," *Radio Science Journal of Research NBS/USNC-URSI*, vol. 68D, no. 2, pp. 239–250, 1964.

[11] Z. M. Zurada, *Introduction to Artificial Neural Systems*, PWS Publishing Company, 1995.

[12] T. S. Rappaport, *Wireless Communications: Principles and Practice*, Prentice Hall PTR, 1996.

[13] C. Phillips, D. Sicker, and D. Grunwald, "A survey of wireless path loss prediction and coverage mapping methods," *IEEE Communications Surveys & Tutorials*, vol. 15, no. 1, pp. 255–270, 2013.

[14] K. Bullington, "Radio propagation for vehicular communications," *IEEE Transactions on Vehicular Technology*, vol. 26, no. 4, pp. 295–308, 1977.

[15] T. L. Singal, *Wireless Communications*, Tata McGraw Hill Education Private Limited, 2010.

[16] ITU-R, *Calculation of Free-Space Attenuation, Recommendation ITU-R P.525-3*, 2016.

[17] D. W. Marquardt, "An algorithm for least-squares estimation of nonlinear parameters," *Journal of the Society for Industrial and Applied Mathematics*, vol. 11, no. 2, pp. 431–441, 1963.

[18] H. Demuth, M. Beale, and M. Hagan, *Neural Network Toolbox*, Mathworks, Natick, MA, USA, 2009.

[19] M. T. Hagan and M. B. Menhaj, "Training feedforward networks with the Marquardt algorithm," *IEEE Transactions on Neural Networks*, vol. 5, no. 6, pp. 989–993, 1994.

[20] J. Milanovic, S. Rimac-Drlje, and I. Majerski, "Radio wave propagation mechanisms and empirical models for fixed wireless access systems," *Technical Gazette*, vol. 17, no. 1, pp. 43–52, 2010.

[21] F. S. Silva, L. J. Matos, F. A. C. Peres, and G. L. Siqueira, "Coverage prediction models fitted to the signal measurements of digital TV in Brazilian cities," in *2013 SBMO/IEEE MTT-S International Microwave & Optoelectronics Conference (IMOC)*, pp. 1–5, Rio de Janeiro, Brazil, August 2013.

[22] M. Yang and W. Shj, "A linear least square method of propagation model tuning for 3G radio network planning," in *2008 Fourth International Conference on Natural Computation*, pp. 150–154, Jinan, China, October 2008.

[23] S. Kim, B. J. Guarino, T. M. Willis et al., "Radio propagation measurements and prediction using three-dimensional ray tracing in urban environments at 908 MHz and 1.9 GHz," *IEEE Transactions on Vehicular Technology*, vol. 48, no. 3, pp. 931–946, 1999.

[24] S. R. Saunders and A. A. Zavala, *Antennas and Propagation for Wireless Communication Systems*, John Wiley & Sons, 2nd edition, 2007.

[25] C. L. Giovanelli, "An analysis of simplified solutions for multiple knife-edge diffraction," *IEEE Transactions on Antennas and Propagation*, vol. 32, no. 3, pp. 297–301, 1984.